AD-A132 283 APPLICATION OF PSEUDOINVERSION TO LINEAR SYSTEM IDENTIFICATION WITH DISCR..(U) MASSACHUSETTS INST OF TECH LEXINGTON LINCOLN LAB C CHANG ET AL. 15 JUL 83 TR-629 ESD-TR-83-038 F19628-80-C-0002 F/G 9/4 NL

1/1

UNCLASSIFIED

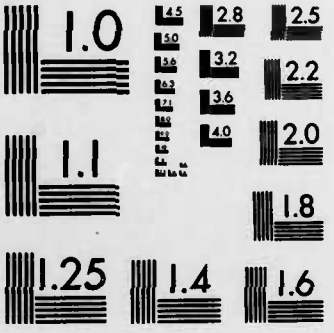

MICROCOPY RESOLUTION TEST CHART
NATIONAL BUREAU OF STANDARDS-1963-A

ESD-TR-83-038

Technical Report	629

Application of Pseudoinversion to Linear System Identification with Discrete Measurements

C.B. Chang
R.B. Holmes

15 July 1983

Prepared for the Department of the Army
under Electronic Systems Division Contract F19628-80-C-0002 by

Lincoln Laboratory
MASSACHUSETTS INSTITUTE OF TECHNOLOGY
LEXINGTON, MASSACHUSETTS

The work reported in this document was performed at Lincoln Laboratory, a center for research operated by Massachusetts Institute of Technology. This program is sponsored by the Ballistic Missile Defense Program Office, Department of the Army; it is supported by the Ballistic Missile Defense Advanced Technology Center under Air Force Contract F19628-80-C-0002.

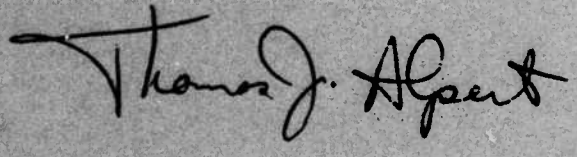

Thomas J. Alpert, Major, USAF
Chief, ESD Lincoln Laboratory Project Office

MASSACHUSETTS INSTITUTE OF TECHNOLOGY
LINCOLN LABORATORY

APPLICATION OF PSEUDOINVERSION TO LINEAR SYSTEM IDENTIFICATION WITH DISCRETE MEASUREMENTS

C.B. CHANG
R.B. HOLMES
Group 32

TECHNICAL REPORT 629

15 JULY 1983

LEXINGTON MASSACHUSETTS

ABSTRACT

Formulas for the pseudoinverse of a compact operator are applied to linear system identification and scattering function estimation from a finite set of noisy measurements. The result is a nonparametric estimator possessing several desirable features. The approach encompasses the Modified Discrete Fourier Transform and is applied herein to the important problem of closely spaced object resolsution in radar/optical siqnal processing.

CONTENTS

I. INTRODUCTION

Extracting information from noisy measurements is a classical problem. Yet, it is this very type of problem which forms a long string of applications challenging engineers and scientists of the past, the present, and likely a long term future. One problem area involves situations wherein an unknown function (signal) is observed after obscuration by a system characterized by a known impulse response and additive random distrubances. With the ever popular digital computing machine, the measurements are recorded digitally. One therefore faces the problem of recovering an unknown continous function from a finite set of discrete measurements.

Motivated by problems in radar/optics scattering function estimation and signal processing, we study a solution to the above problem in this paper. Let s(t) denote the transmitted signal of a radar (or communication) system. This signal is scattered by a target (or channel) represented by a linear system with impulse response x(t) which we shall call the "scattering function". The waveform at the front end of the receiver is the convolution of x(t) and s(t). Let the receiver be a conventional matched filter with impulse response matched to the transmitted signal, the receiver output being therefore a double convolution denoted as s(t)*(s(t)*x(t)). We

further assume that the received data is recorded in sampled form. Given the sample data set, $y(t_i)$, $i=1,\ldots,n$, we would like to estimate the target configuration (or channel property) represented by the scattering function $x(t)$. In the context of linear system identification, the above problem is the same as the problem of estimating the impulse response (or input signal) of a linear system given the input signal (or system impulse response) and the discrete samples of the output of the linear system.

Typical approaches to problems of this kind fall into two distinct categories. The first one is to treat it as a deconvolution problem. In this case the convolution integral is approximated with a convolution summation, and the deconvolution procedure is carried out either via the discrete Fourier transform or directly in the time domain, as in [2]. The second approach is to utilize a parametric model of the unknown signal $x(t)$ and attempt to estimate parameter values embedded in the $x(t)$ model. One example in the radar/optics area is the resolution of closely spaced objects. In this case a maximum likelihood estimator is used to estimate target amplitudes and locations for an assumed number of targets contained in the observation. In the latter part of this report we will use the closely spaced object resolution problem an an example of comparison between our approach and the

parametric estimator described above.

The method to be described in this report is a nonparametric estimator. It is derived using the pseudoinversion concept of operator theory. Our method is similar to the deconvolution method in that both utilize a nonparametric approach and both are solving an integral equation. Our approach does not, however, require the approximation of convolution integral by a summation and furthermore, the estimator is a continuous time function even though the data is given in sampled form. Our estimator therefore possesses the combined features of deconvolution and interpolation.

We summarize features of our approach below. The process of the radar/communicaton problem described above can be viewed as a composite linear transformation between a time function $x(t)$ of a Hilbert space H and sampled data $y(t_i)$, $i=1,\ldots,n$, of a n-dimensional Euclidean space E^n. This composite operator consists of convolution integral operators with kernels $s(t)$ and the sinc function. Let $Q: H \to E^n$ denote this operator, then one can write,

$$y = Qx \tag{1.1}$$

where $x(t) \in H$ and $y \in R(Q) \subset E^n$, the sampled data array. Notice that we use $R(\cdot)$ to denote the range space of the enclosed operator. Letting Q^+ denote the pseudoinverse of Q, our

estimate $\hat{x}(t)$ of $x(t)$ is given by

$$\hat{x} = Q^{+}\underline{y}. \tag{1.2}$$

The estimate $\hat{x}$ possesses several desirable properties:

(1) It has least norm among all elements of H whose Q-image agrees with y; hence $\hat{x}$ has an interpolating spline significance.

(2) When a prior bound on $||x||$ is given, $\hat{x}$ minimizes the maximum error subject to this bound; hence $\hat{x}$ has a minimax significance.

(3) More generally, if $T:H\to K$ is another operation into a Hilbert space K, then $T(\hat{x})$ is the best (minimax) estimate of $T(x)$, given the data y and a prior bound on $||x||$. (The case where T is the Fourier transform is of particular interest).

In this report we will describe the theory leading to representations of the pseudoinverse Q^{+} and formulas for $\hat{x}$. This operator theory is next applied in Chapter 3 to the problem described above. Finally, three examples are considered in Chapter 4. The first of these is simple pointwise interpolation from a finite set of sample values. The resulting formula is the time-domain version of the Modified Discrete Fourier Transform of [3]. The second example illustrates noise-free reconstruction of a truncated sinusoid. The last (and most serious) example concerns the problem of closely spaced object resolution, wherein the original signal x is modeled as an impulse train. The performance of our method on noisy data is discussed and illustrated by several figures.

II. REVIEW OF RELEVANT OPERATOR THEORY

Let $Q: H_1 \to H_2$ be a compact linear operator on the Hilbert space H_1 with range $R(Q)$ in the Hilbert space H_2. With Q^+ denoting the pseudoinverse of Q, our estimate x of the solution x to the equation

$$y=Q(x) \tag{2.1}$$

is

$$\hat{x} = Q^+(y) \tag{2.2}$$

In section 2.1 below we briefly review general properties of Q and Q^+. In section 2.2 we focus on the important special case where Q is of finite rank; this includes the situations where the data vector y consists of sampled values.

2.1 Structure of Compact Operators and Their Pseudoinverses

We begin by recalling the basic structure of a compact self-adjoint ($Q=Q^*$) operator.

Theorem 2.1 (Spectral Theorem) Let Q be a compact self-adjoint operator acting on a Hilbert space H. Then the non-zero spectrum of Q has the form $\{\lambda_1, \lambda_2, \ldots\}$ where each λ_j is a real eigenvalue of finite multiplicity, and $\lim \lambda_j=0$ if H is of infinite dimension. There is a corresponding orthonormal sequence $\{e_j\}$ of eigenvectors such that

$$Q(x) = \sum_j \varepsilon_j \langle x, e_j \rangle e_j, \quad x \in H \tag{2.3}$$

Corollary 2.1.1 (Resolution of the Identity) With Q as above, let P_j be the orthogonal projection of H onto span $\{e_j\}$. Then

$$\begin{aligned} &\text{i)} && \sum P_j = I \qquad \text{(strong convergence)} \\ &\text{ii)} && P_j P_k = P_k P_j = \delta_{kj} P_j \\ &\text{iii)} && \sum \lambda_j P_j = Q \qquad \text{(norm convergence)} \end{aligned} \tag{2.4}$$

This result shows that Q can be synthesized from real linear combinations of commuting orthogonal projections.

Corollary 2.1.2 (Characterization of the Range) With Q as above, a necessary and sufficient condition that y belong to R(Q) is

$$\begin{aligned} &\text{i)} && y \perp N(Q), \text{ the nullspace of Q, and} \\ &\text{ii)} && \sum \lambda_j^{-2} \left| \langle y, e_j \rangle \right|^2 < \infty \end{aligned} \tag{2.5}$$

If so, then all preimages of y have the form

$$x = u + \sum \frac{\langle y, e_j \rangle}{\lambda_j} e_j, \tag{2.6}$$

for any $u \in N(Q)$.

Theorem 2.1 and its corollaries are standard; their proofs may be found, for example, in [1]. Equation (2.6) in effect specifies the complete (multivalued) inverse of Q. When

we use

$$\hat{x} = \sum \frac{\langle y, e_j \rangle}{\lambda_j} e_j \tag{2.7}$$

as the estimate for x, we recover the component of x that is orthogonal to N(Q).

These results are not generally of immediate applicability because of the self-adjointness requirement. We can, however, use them to establish analogues of the expansions (2.3) and (2.6) for arbitrary compact operators.

Theorem 2.2 (Singular Value Decomposition) Let $Q: H_1 \to H_2$ be a compact operator acting between the Hilbert spaces H_1 and H_2. Then there are orthonormal bases $\{u_n\}$ of $N(Q)^{\perp}$ and $\{v_n\}$ of $\overline{R(Q)}$ such that

$$Q(x) = \sum_j \sigma_j \langle x, u_j \rangle v_j, \quad x \in H_1 \tag{2.8}$$

Hence $\{\sigma_1^2, \sigma_2^2, \ldots\}$ is the non-zero spectrum of QQ^* (or, Q^*Q).

The positive numbers $\sigma_1, \sigma_2, \ldots$ are termed the singular values of Q. Theorem 2.2 generalizes the familiar matrix singular value decomposition

$$A = VDU^* \tag{2.9}$$

where A is arbitrary, U and V are unitary, and D is a non-negative diagonal matrix. The decomposition (2.9) is easily

seen to imply the polar decomposition

$$A = UR \tag{2.10}$$

where U is unitary and R is positive semidefinite. Conversely (2.10) combined with the Spectral Theorem yields a simple proof of (2.9), and (2.8) may similarly be obtained from Theorem 2.1 and the general polar decomposition for operators.

Corollary 2.2.1 (Characterization of the Range) With the notations of the preceding theorem, a necessary and sufficient condition that $y \in R(Q)$ is

i) $y \perp N(Q^*)$, and

ii) $$\sum \sigma_j^{-2} \left|\langle y, v_j \rangle\right|^2 < \infty \tag{2.11}$$

Inequality ii) of the corollary is often called the Picard Condition. Vectors y obeying it constitute the domain $D(Q^+)$ of the pseudoinverse Q^+ of Q:

$$D(Q^+) = R(Q) + N(Q^*)$$

$$= \{y \in H_2 : \min \left|\left|Q(x)-y\right|\right| \text{exists in } H_1\}.$$

Any x minimizing $\left|\left|Q(x) - y\right|\right|$ is called an extremal solution of equation (2.1). There is a unique extremal solution of least norm; this is the vector

$$\hat{x} = Q^+(y) = \sum \frac{\langle y, v_j \rangle}{\sigma_j} \, u_j \tag{2.12}$$

This last formula defines the pseudoinverse operator Q^+ on

its domain $D(Q^+)$. We see that, unless $R(Q)$ is a closed subspace of H_2 (which, for compact Q, happens iff Q is of finite rank), Q^+ is defined only on a dense linear subspace of H_2 and is an unbounded operator. In this case equation (2.1) is ill-posed even if Q is one-to-one and there will be an inherent ill condition in any inversion attempt.

Although of limited paractical value because of the difficulty in knowing all the singular values σ_j, formula (2.12) is extremely important theoretically as a device for analyzing the pseudoinverse solution. First of all, it demonstrates the precise source of ill conditioning by showing that any perturbation of y in the v_j direction is magnified by the factor σ_j^{-1}, which can be arbitrarily large. Secondly, the convergence of numerous iterative and regularization schemes for equation (2.1) can be viewed as particular cases of a "filtered" pseudoinversion wherein the factors σ_j^{-1} in (2.12) are replaced by new factors $\phi(\sigma_j)$. Here the non-negative function $\phi(t)$ vanishes at 0 and behaves asymptotically as t^{-1} for $t \to +\infty$. In particular when ϕ vanishes on an interval $[0, \delta]$ we have a "truncated" pseudoinversion.

2.2 Operators of Finite Rank and Their Pseudoinverses

When measurements of a signal occur discretely (the

sampled data case) our observation operator Q has range in E^n and hence is of finite rank. There is, of course, in general a fundamental dichotomy for compact operators according as they have closed range (and hence finite rank) or not. We recall in the following proposition standard properties of the pseudo-inverse of any operator with closed range.

Proposition 2.1 Let $Q: H_1 \to H_2$ be a bounded linear operator with range closed in H_2, and let Q^+ be its pseudoinverse. Then

a) $Q^+: H_2 \to H_1$ is bounded

b) $(Q^+)^+ = Q$

c) $Q^+QQ^+ = Q^+$

d) $QQ^+Q = Q$

e) QQ^+ = orthogonal projection on $R(Q)$

f) $I-Q^+Q$ = orthogonal projection on $N(Q)$

It follows from part f) that Q^+Q is the orthogonal projection of H_1 on $N(Q)^\perp$ and hence that Q^+ maps $R(Q)$ (indeed, all of H_2) onto $N(Q)^\perp$. With reference to equation (2.1) we may say, when $R(Q) = H_2$ (as may be assumed when Q is of finite rank), that Q^+ recovers the component of x in $N(Q)^\perp$, although, strictly speaking, Q^+ does not "know" about x. Equivalently, $Q^+(y)$ is the element of least norm in the variety $\{x \in H_1: Q(x)=y\}$ and, as such, has an interpolating spline significance.

That is, if "smoothness" of elements of H_1 can be thought of as varying inversely with the size of the norm on H_1, then $Q^+(y)$ is the smoothest interpolant in H_1 of the data y. This remark is particulary pertinent when H_1 is a reproducing kernel or functional Hilbert space.

Another interpretation of the estimate $\hat{x} = Q^+(y)$ is possible when a prior bound on $||x||$ is given in addition to equation (2.1). Then it is not hard to see that $\hat{x}$ minimizes the maximum error (as measured by the norm on H_1) subject to this bound. Precisely, x is the center of the "hypercircle" in H_1 defined by the data and the prior bound. Thus $\hat{x}$ has a minimax significance.

The next result leads to the fundamental formula for Q^+ in the finite rank case. With it we can bypass formula (2.12) and reduce to a matrix inversion.

Theorem 2.3 a) Let $Q:H_1 \to H_2$ be any bounded operator with closed range. Then a)

$$Q^+ = Q^*(QQ^*)^+ \tag{2.13}$$

b) If $R(Q) = H_2$ then QQ^* is invertible and so

$$Q^+ = Q^*(QQ^*)^{-1}. \tag{2.14}$$

Part a) of the Theorem can be proved by first noting that $N(QQ^*) = N(Q^*)$ and hence that $R(QQ^*) = R(Q)$, since $R(Q)$ is closed. Next both sides of (2.13) are seen to annull $N(Q^*) = R(Q)^{\perp}$. Finally, using the invertibility of Q on $N(Q)^{\perp}$ one shows that the right side of (2.13) agrees with this inverse on $R(Q)$. Part b) is immediate.

It remains to identify the operators appearing on the right side of (2.14) when Q has finite rank. In this case we may assume that $R(Q) = E^n$ where $n = \text{rank}(Q)$. If $\{e_1,\ldots,e_n\}$ is the standard unit vector basis in E^n, there exists elements $\{q_1,\ldots,q_n\}$ (not necessarily orthonormal) in H_1 such that

$$Q(x) = \sum_{j=1}^{n} \langle x,q_j\rangle e_j, \quad x \in H_1 \tag{2.15}$$

Note that (2.15) is not generally the singular value decomposition of (2.8), but rather is chosen for convenience in problem formulation. If, in fact, the expansion (2.8) is known then, as we have seen, Q^+ is directly given by (2.12).

Proposition 2.2 With Q given in the form (2.15) we have

$$Q^*(y) = \sum_{j=1}^{n} \langle y,e_j\rangle q_j,$$

and the matrix of

$$QQ^* = [\langle q_j, q_i \rangle], \tag{2.16}$$

relative to the basis $\{e_1, \ldots e_n\}$.

It follows that for $y = (y_1, \ldots, y_n)^T \in E^n$,

$$Q^+(y) = \sum_{j=1}^{n} \lambda_j q_j, \tag{2.17}$$

with

$$[\langle q_j, q_i \rangle] \lambda = y. \tag{2.18}$$

The matrix appearing in (2.16) and (2.18) is the transposed Gram matrix of the vectors $\{q_1, \ldots, q_n\}$ and is exactly the Gram matrix when the underlying scalars are real. As such, this matrix is positive definite, although possibly ill-conditioned, the latter depending on the relative lengths and alignments of the vectors q_j in H_1.

When ill-conditioning is present and there is noise in the data vector y, recourse may be had to a regularization of the pseudoinverse. In this case the coefficients λ_j in (2.17) are replaced by λ_j^ε where $\varepsilon > 0$ and λ^ε satisfies

$$(QQ^* + \varepsilon I)\lambda^\varepsilon = y. \tag{2.19}$$

The corresponding solution in H_1 then has a smoothing spline interpretation; it varies in $N(Q)^\perp$ between $Q^+(y)$ (for $\varepsilon \to 0$)

and the zero vector (for $\varepsilon \to \infty$). This procedure is equivalent to a particular choice of the filtering functions ϕ that were introduced at the end of section 2.1 in the context of pseuo-inversion via singular value decomposition. Namely,

$$\phi(x) = \frac{x}{x^2+\varepsilon}.$$

Some examples of the use of such regularized pseudoinversions are given in section 4.3 below.

III. THE PROBLEM OF LINEAR SYSTEM IDENTIFICATION/SCATTERING FUNCTION ESTIMATION

We now apply the results of Section 2 to the problem of linear system identification. We will still use the scattering function estimation problem as a guideline in formulating the composite operator. The linear system identification problem is clearly contained in this problem area.

3.1 The Composite Operator

As discussed before, the output of a radar receiver can be written in terms of a double integral,

$$y(t) = \int d\tau_1 s(t-\tau_1) \int d\tau_2 s(\tau_1-\tau_2) x(\tau_2) \qquad (3.1)$$

where $x(\cdot)$ is the scattering function to be estimated and $s(\cdot)$ is the transmitted signal*. The output $y(t)$ is then sampled to obtain the discrete data $y(t_i)$, $i=1\ldots,n$. We can represent the sampling process using a reproducing kernel (RK) $K(t,\tau)$ where

$$K(t,\tau) = \text{sinc}(\Omega(t-\tau))$$

$$= \frac{\sin(\Omega(t-\tau))}{\pi(t-\tau)} \qquad (3.2)$$

*For the purpose of simplicity, we avoid the representation of radar signals using complex functions.

The bandwidth, Ω, is dictated by the bandwidth of y(t) (not x(t)). Notice that $K(t,\tau)$ is a RK because sinc $(\cdot)$ is a function of positive type (its Fourier transform is nonnegative); hence

$$y(t) = \langle K(t,\cdot),\ y(\cdot)\rangle \tag{3.3}$$

whenever y is Ω-bandlimited. In particular,

$$y_i \overset{\Delta}{=} y(t_i) = \int K(t_i,\tau)y(\tau)d\tau. \tag{3.4}$$

Assuming that s(t) is symmetric about its mean and letting $\rho(t)$ denote the autocorrelation function of s(t), one then has

$$\rho(t) = \int s(t-\tau)s(\tau)\ d\tau \tag{3.5}$$

Combining Eqs. (3.2), (3.4), and (3.5), one obtains

$$y_i = \int \rho(t_i-\tau)x(\tau)d\tau \tag{3.6}$$

for i=1,...,n.

Applying equation (2.15) to (3.6), one obtains

$$Q = \begin{bmatrix} \langle\ ,\ \rho_1\rangle \\ \vdots \\ \langle\ ,\ \rho_n\rangle \end{bmatrix} \tag{3.7}$$

where $\rho_i=\rho(t_i-\tau)$ and the inner product is specified by (3.6)

It is now clear that Q is a mapping from L^2 to E^n.

Given y_i, i=1,...,n, to find x(t) is a problem of mapping from E^n to L^2. Equation (3.6) also clearly indicates that this is the same problem as the linear system (or input) identification (or estimation) problem.

3.2 The Adjoint Operator

Using proposition 2.2, one obtains

$$Q^*(y) = \sum_{i=1}^{n} y_i \rho_i \tag{3.8}$$

or

$$Q^* = [\rho_1, \ldots, \rho_n] \tag{3.9}$$

Notice that the right side of equation (3.7) is a column vector where each component is a functional represented by an inner product. The adjoint Q^* maps, however, from sampled data space E^n back to a space L^2 of functions of continuous time, Equations (3.8) and (3.9) clearly reflect this fact since ρ_i is a function of continuous time.

3.3 The Pseudoinverse Operator

Applying the above results to Eq. (2.14), the pseudo-inverse operator readily follows:

$$Q^+ = Q^*(QQ^*)^{-1}$$

$$= [\rho_1, \ldots, \rho_n][<\rho_i, \rho_j>]^{-1} \tag{3.10}$$

where $\langle \rho_i, \rho_j \rangle$ is the (i,j)th component of the n by n matrix of (QQ^*) and

$$\langle \rho_i, \rho_j \rangle = \int \rho(t_i - \tau)\, \rho(t_j - \tau)\, d\tau \qquad (3.11)$$

In the problem of radar scattering function estimation, $\rho(t)$ is the autocorrelation function of the transmitted signal, and is therefore symmetric about t=0. In the context of linear system identification and input estimation, $\rho(t)$ is either the system inpulse response or the input signal used to probe the unknown system, and is usually a nonsymmetric function of time. In any event, the matrix of $(QQ^*)^{-1}$ can be pre-computed and its function is simply to weight the data vector $\underline{y}$. Let $\underline{a}$ denote the weighted data vector, i.e.,

$$\underline{a} = (QQ^*)^{-1}\underline{y} \quad ; \qquad (3.12)$$

then the final estimate of x takes the form

$$\hat{x}(\tau) = Q^+\underline{y}$$

$$= \sum_{i=1}^{n} \rho(t_i - \tau)\, a_i \qquad (3.13)$$

Notice again that the estimate $\hat{x}(\tau)$ is a function of continuous time τ.

The conventional approach to the problem of decon-

volution is to first approximate the convolution integral with a summation. In our problem, although the data is recorded in discrete form, the estimate can be evaluated at any instant of time. Our method includes therefore both deconvolution and interpolation. We will apply the interpolation significance of our approach to present an interpolation formula for finite number of samples in the example section.

3.4 Discussion of Numerical Problems

Since the computation of Q^+ involves a matrix inversion, numerical problems may become an issue. This can be made clear by examining Eq. (2.12). When the condition number ($\triangleq$ the ratio of the largest to the smallest eigenvalue) of QQ^* approaches the dynamic range of the digital computer used for implementation, its inverse can no longer be represented exactly. In addition, even before the condition number approaches the range of a computer, a slight disturbance in y (e.g., measurement noise) will be amplified by the small eigenvalues (see Eq. (2.12)). Methods for reducing such effects are therefore of practical importance.

Among these methods are the truncated and regularized pseudoinverse already mentioned in Section 2, where it was also noted that both methods are special cases of a filtered pseudoinversion obtained by replacing σ_j^{-1} in (2.12) by $\phi(\sigma_j)$.

Each of these methods involves a trade-off between fidelity to the data and noise suppression. As we insist on greater fidelity we amplify the noise transmitted to the solution, and conversely. The final choice of trade-off may be made either on the basis of prior knowleldge of noise statistics or interactively.

For example, the truncated singular value estimate $\hat{x}_\delta$ is obtained from (2.12) by deleting those terms in the sum for which $\sigma_j < \delta$; thus

$$\hat{x}_\delta = \sum_{\sigma_j \geq \delta} \frac{\langle y, v_j \rangle}{\sigma_j} u_j. \tag{3.14}$$

This is equivalent to the ordinary singular value pseudoinverse applied to the projection of the data onto span $\{v_j: \ \sigma_j \geq \delta\}$. A key point here is that the method is independent of the data y, depending only on the singular system of the operator Q. Hence if the noise has large components along the remaining σ_j directions in (3.14), there is unavoidable trouble. When it can be assumed that y includes an additive white noise perturbation with known variance s^2, then a common approach is to chose the largest δ that makes the residual $\left|\left|Q(\hat{x}_\delta)-y\right|\right| < [\text{rank } (Q)]^{1/2} \cdot s$.

The regularized estimates $\hat{x}_\varepsilon$ were defined through

Eqs. (2.17) and (2.19):

$$\hat{x}_\varepsilon = \sum_{j=1}^{n} \lambda_j^\varepsilon q_j. \tag{3.15}$$

It was noted that while x_ε could be viewed in terms of filtering the singular value expression (2.12) for $Q^+(y)$, for computational purposes this expansion is not required to be known.

The estimate x_ε can alternatively be viewed as the minimizer of the function

$$||Q(x) - y||^2 + \varepsilon||x||^2. \tag{3.16}$$

In particular, when the measurement vector is corrupted with additive noise with covariance R, a weighted minimum norm solution is sought, i.e.,

$$||Q(x) - y||^2_{R^{-1}} + \varepsilon||x||^2 \tag{3.17}$$

This results in the following expression for λ^ε,

$$L(L^{-1}QQ^*L^{-T} + \varepsilon I)L^T\lambda^\varepsilon = y \tag{3.18}$$

where $LL^T \triangleq R$, as opposed to (2.19). In this case, (3.15) and (3.18) give the regularized estimate $\hat{x}_\varepsilon$.

Regularization is closely related to the "ridge regression" method of statistics, except that the rank assumptions on the observation operator Q are somewhat

different in that context. Intuitively, one replaces an initial ill-conditioned inversion problem $Q(x)=y$ by a neighboring well-conditioned problem $Q_\varepsilon(x) = y$, solves this for $\hat{x}_\varepsilon$ and then verfies $\lim \hat{x}_\varepsilon = Q^+(y)$ as $\varepsilon \to 0$. As such, regularization is one type of representation of the pseudoinverse Q^+. This latter topic has been extensively studied for general bounded operators [4].

A good discussion of the relative merits of truncated and regularized pseudoinversion, particularly with respect to the noise level in the data is given in [5].

In the next section, three examples will be presented. The last example deals with the closely spaced object resolution problem where noisy measurements will be used. Numerical problems mentioned above will be further examined, and the results of applying the regularization method will be studied. The criterion for choosing the value of the regularization coefficient is in terms of a desired false alarm probability.

IV. EXAMPLES

Three examples are presented in this section. In the first example, we apply the theory of Section 3 to derive an interpolation formula for finite number of samples, i.e., given $z(t_i)$, $i=1,\ldots,n$, find $\hat{z}(t)$ for $t \in (-a,b)$ where a and b can be arbitrarily large. In the second example, we use a truncated sine function as the scattering function and demonstrate the reconstructed function. The third example deals with the problem of resolving closely spaced targets (signals).

4.1 A Formula for Interpolation With Finite Number of Samples

Let $z(t)$ be a bandlimited function defined as

$$z(t) \in BL(\Omega)$$

$$\triangleq \{z(t) \in L^2(-\infty,\infty): \; Z(w)=0 \text{ (a.e.) for } |w|>\Omega\} \qquad (4.1)$$

where $Z(w)$ is the Fourier transform of $z(t)$.

From Eq. (3.3) the sampling operation is represented by the reproducing kernel $K(t,\tau)$ given in (3.2), that is,

$$K(t,\tau) = \frac{\Omega}{\pi} \operatorname{sinc}(\Omega(t-\tau)), \qquad (4.2)$$

and the samples of $z(t)$ are obtained as

$$z(t_i) = \int K(t_i,\tau)z(\tau)d\tau. \tag{4.3}$$

From (3.10) we have the estimate

$$\hat{z}(\tau) = Q^*(QQ^*)^{-1}\underline{z} \tag{4.4}$$

where $\underline{z} = [z(t_1),\ldots,z(t_n)]^T$

$$Q^* = [K(t_1,\tau),\ldots,K(t_n,\tau)]$$

$$QQ^* = [\langle K(t_i,\tau),\ K(t_j,\tau)\rangle]$$

$$= [K(t_i,t_j)].$$

Suppose that the samples are spaced using the "Nyquist" rate, i.e.,

$$t_{i+1}-t_i = \frac{\pi}{\Omega} = \text{a constant},$$

then

$$\langle K(t_i,\tau),\ K(t_j,\tau)\rangle = \frac{\Omega}{\pi}\,\delta_{ij}, \tag{4.5}$$

where δ_{ij} is the Kronecker delta function. We therefore have QQ^* a diagonal matrix, or

$$\hat{z}(\tau) = \sum_{i=1}^{n} z(t_i)\ \mathrm{sinc}(\Omega(t_i-\tau)) \tag{4.6}$$

If the samples are, however, taken other than (faster or slower) the Nyquist rate, QQ^* is no longer a diagonal

matrix. Let r_{ij} denote the (i,j)th entry of $(QQ^*)^{-1}$ and $\underline{a} = (QQ^*)^{-1}\underline{z}$, then

$$a_i = \sum_{k=1}^{n} r_{ik} z(t_k) \tag{4.7}$$

Hence, the interpolated z(t) is

$$\hat{z}(\tau) = \sum_{i=1}^{n} a_i \sin(\Omega(t_i - \tau))$$

$$= \sum_{i=1}^{n} \sum_{k=1}^{n} r_{ik} z(t_k) \sin(\Omega(t_i - \tau)) \tag{4.8}$$

Equations (4.6) and (4.8) give an interpolation formula for finite number of samples. We make the following remarks:

1) When sampled at Nyquist rate, the interpolation formula (eq. (4.6)) is the traditional sinc function weighted with samples. Each data sample appears only once.

2) When sampled at other than the Nyquist rate, the samples are first summed with weightings determined by $(QQ^*)^{-1}$. The sinc function at a time instant carries several data samples.

3) The above reconstruction formula (with or without noise corruption) is optimum in the minimax sense (see section 2).

4) The numerical difficulties of this approach, if any, lie in the inversion of QQ^*. If the condition number of QQ^* is too large, an anomolous response begins to occur in the reconstructed function (especially with noisy measurements), and one must resort to such methods as truncated or regularized pseudoinversion as indicated in Section 3.5.

5) The results above have apparently been previously discussed in the literature in the context of the Modified Discrete Fourier Transform (MDFT), [3]. Our results are, however, obtained with an entirely different and more general operator-theoretic approach. In particular, our solution is obtained in the time domain, while that of [3] is obtained as a constrained optimization in the frequency domain.

4.2 A Truncated Sine Function

Let $x(t)$ be a truncated sine function over two cycles, i.e.,

$$\begin{aligned} x(t) &= \sin 2\pi t \quad ; \quad 0 \leq t \leq 2 \\ &= 0 \quad ; \quad \text{otherwise.} \end{aligned} \tag{4.9}$$

We choose a Gaussian shaped function to represent the signal autocorrelation function, i.e.,

$$\rho(t) = e^{-t^2/2} \tag{4.10}$$

There are two reasons for using (4.10). First it is simple to manipulate analytically. Second, it closely approximates the Hamming weighted and compressed linear frequency modulated waveform.

We will only examine the noise-free case for this example. Results are shown in Figs. 4.1 to 4.3 for a total of 9, 17, and 25 samples, respectively. Notice that measurements are taken over the time interval where x(t) is not zero. The solid curve gives the true function. The diamond shaped symbols represent the discrete measurements, y_i, i=1,...,n. The small squares are the estimates. Notice that the higher the number of samples is, the closer the estimates are to the true curve. With only 9 points over a two cycle period, the estimates are still very close to the truth. Since the measurements are obtained as the convolution of x(t) and $\rho(t)$, they do carry information about x(t) outside the measurement interval. This is evident via the fact that the estimates rapidly go to zero as the true function does.

4.3 The Closely Space Object Resolution Problem

We next consider a problem of practical interest in radar and/or optical signal processing. In this example, x(t) becomes a series of impulse function with each impulse

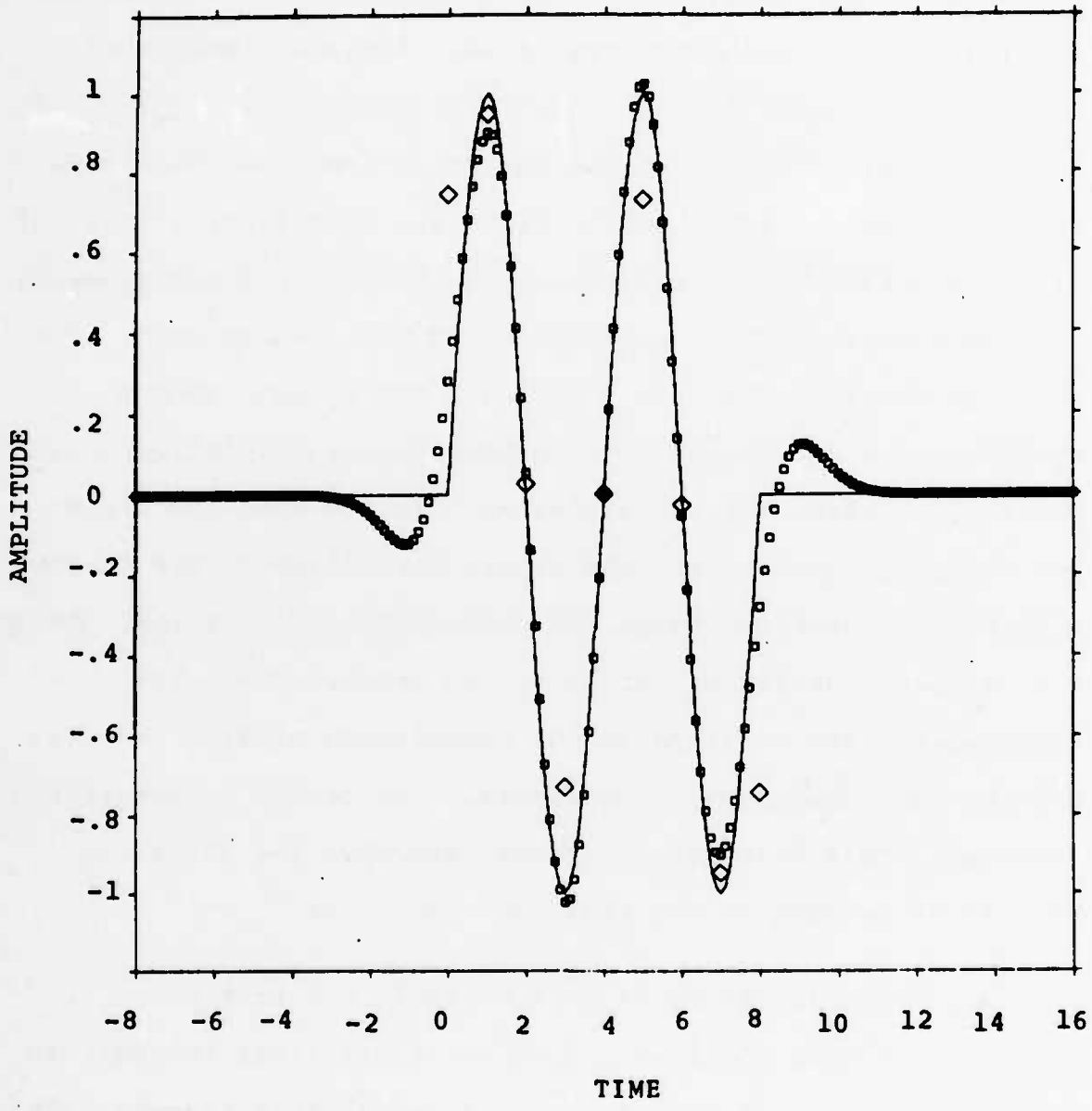

Fig. 4.1. Two-cycle sine with 9 samples.

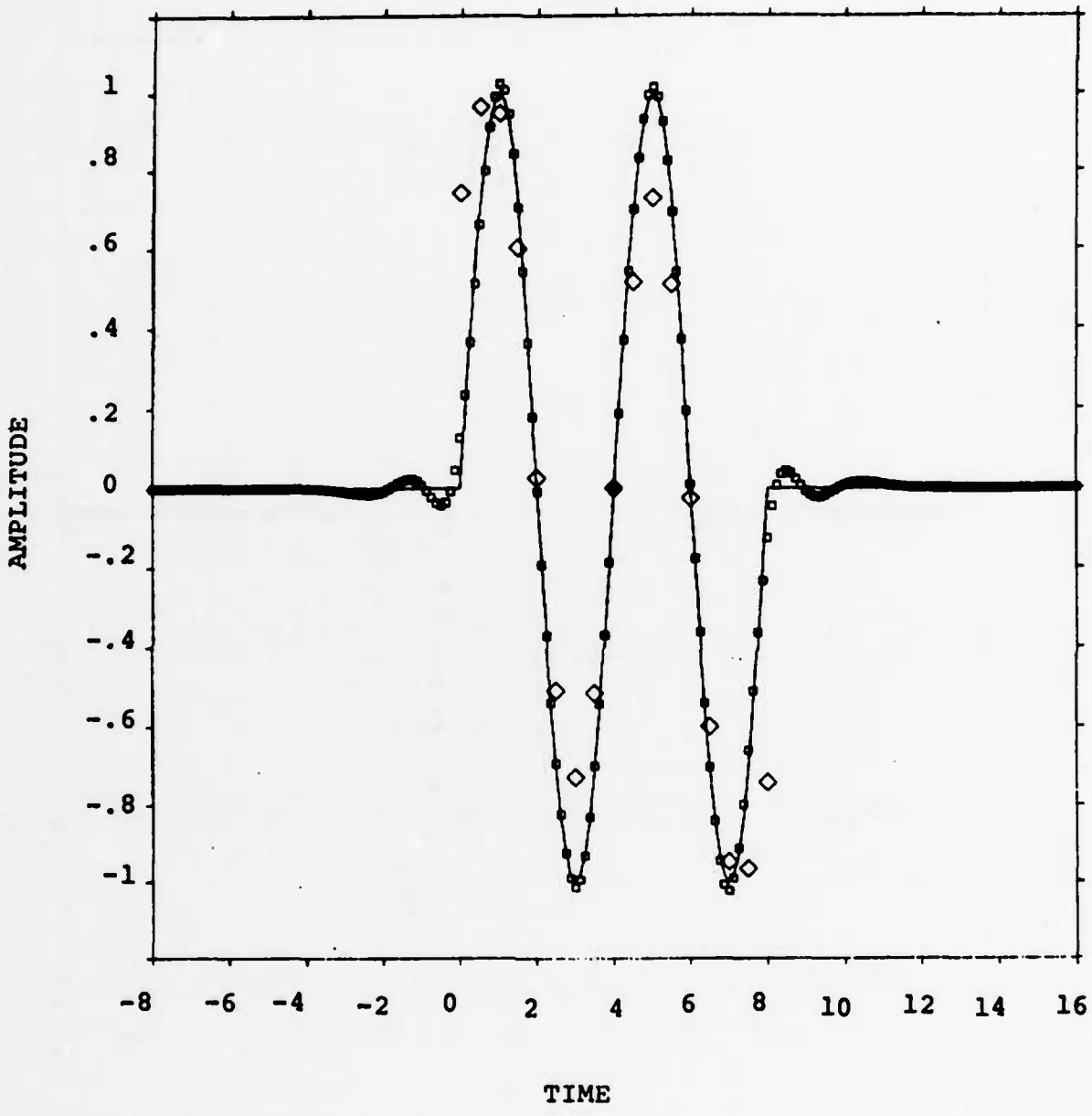

Fig. 4.2. Two-cycle sine with 17 samples.

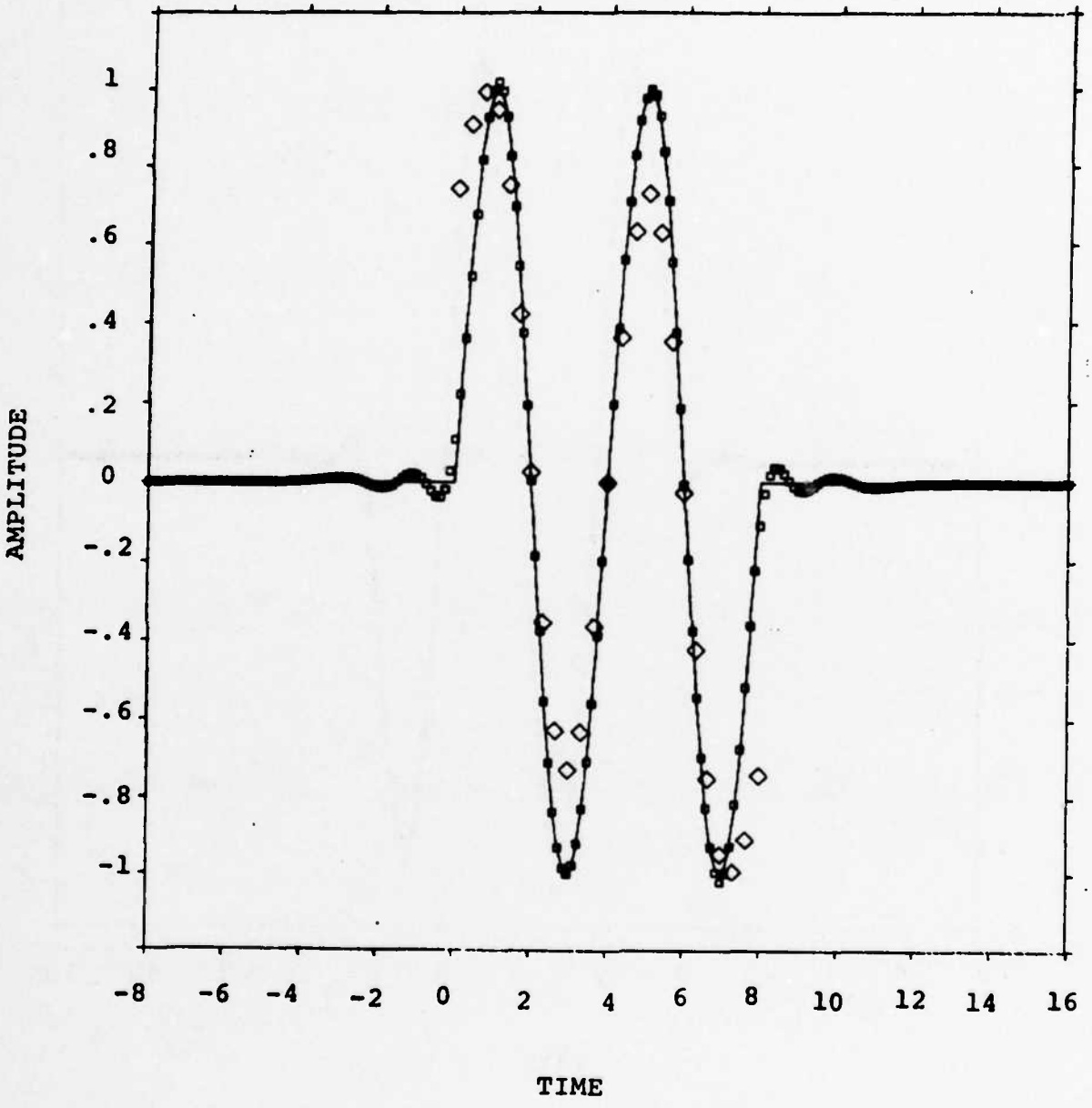

Fig. 4.3. Two-cycle sine with 25 samples.

representing a point target and the magnitude of the impulse giving the signal amplitude.

The Fourier transform of an impulse function has a constant amplitude over all frequencies. The output y(t) may however, be bandlimited as determined by the signal autocorrelation function $\rho(t)$. We use a Gaussian shaped function to represent $\rho(t)$ as shown in Eq. (4.10) Although a Gaussian shaped function is not bandlimitted, we use a $\pm$ 3 standard deviation width of its spectrum to approximate its "bandwidth". Using (4.10), one can quickly obtain the (pseudo) Nyquist sampling interval as $\Delta t \approx 1$.

In Fig. 4.4, we present the noise-free measurements and the estimate of a point target. Notice that the true function is an impulse function represented by a vertical line in Fig. 4.4. The estimated waveform resembles a sinc function. A circle is drawn at the peak of the recovered pulse. Recall that an impulse can be expressed as the limit of a sinc function with its bandwidth approaching infinity. The estimate can be made closer to an impulse if more and denser samples are taken. This gradually introduces numerical problems, however, since the condition number of QQ^* will become large.

In Fig. 4.5, we present the results for two targets separated by 1.5 standard deviations. For radar (optical)

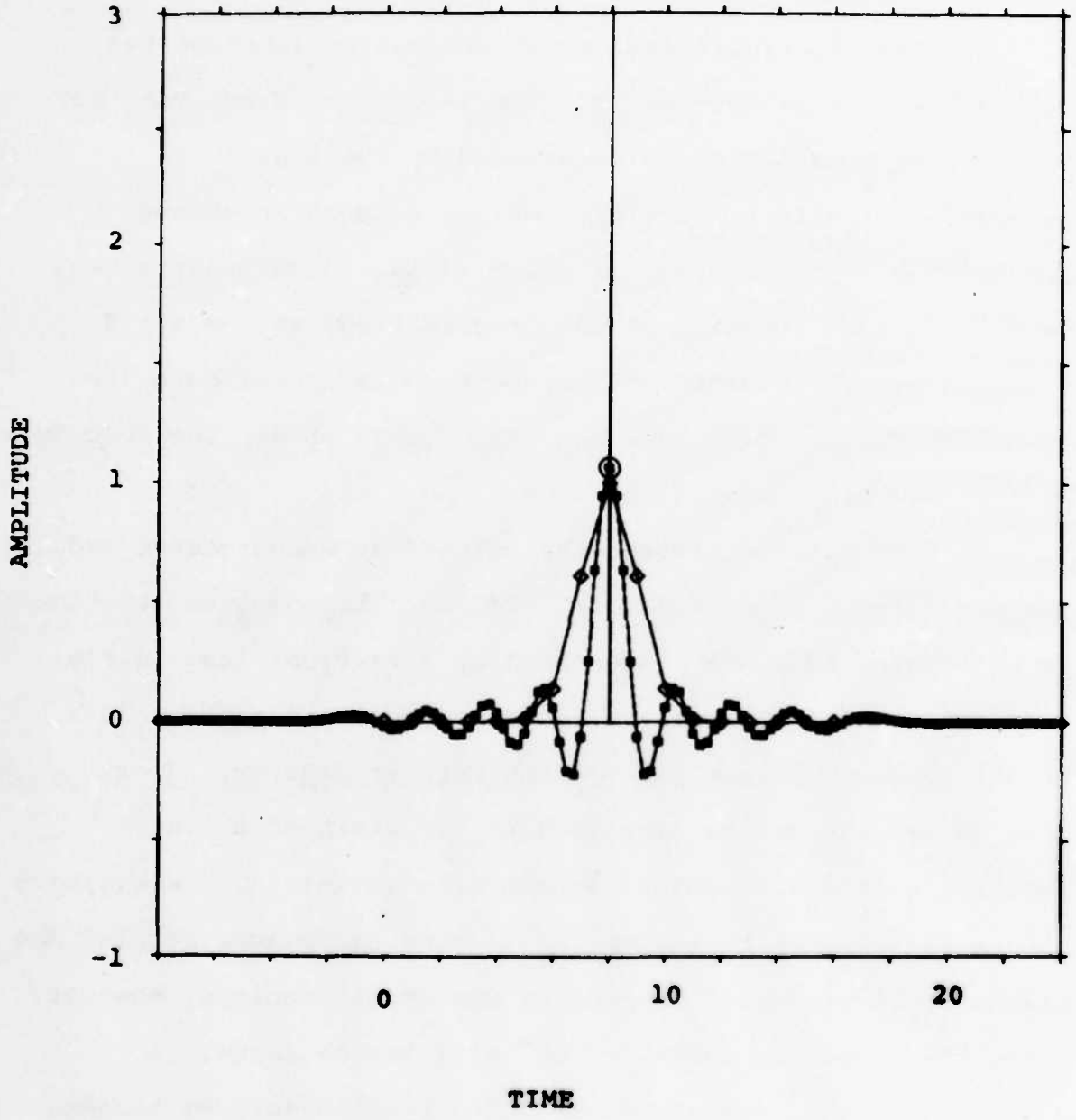

Fig. 4.4. Point target case ($\Delta t=1$).

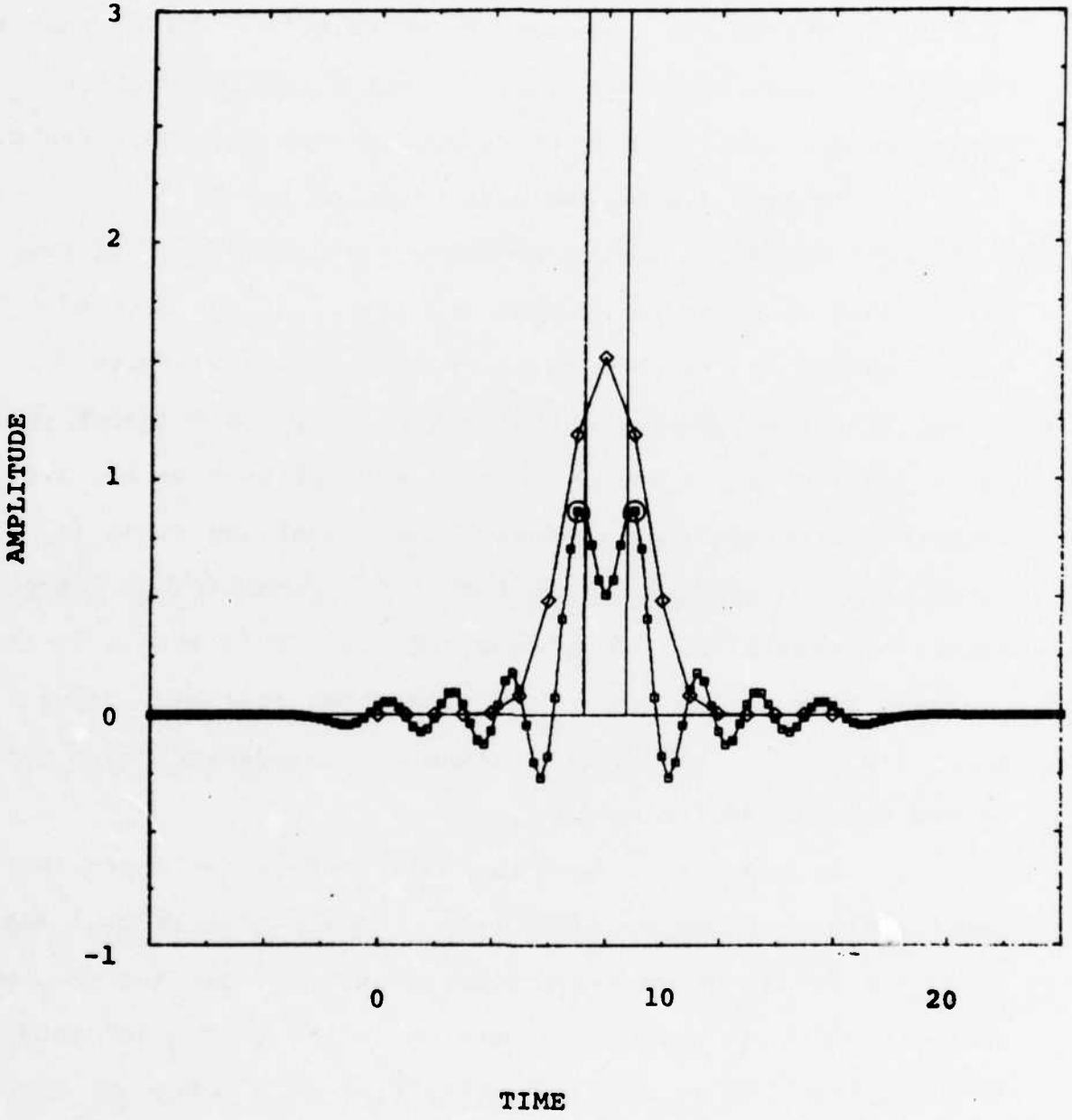

Fig. 4.5. Point target case (separation = 3/4 resolution).

signals, this corresponds to a 3/4 resolution (detector width) separation. In this noise free case, the estimated function clearly indicates the presence of two targets. Notice that the two signal peaks corresponding to the two target location estimates are indicated by two circles enclosing these peaks.

In Fig. 4.6 we add noise samples to the measurements. The noise samples are meant to represent the white additive noise at a radar receiver. At the matched filter output the noise samples become correlated, with correlation function being the same as $\rho(t)$. A signal-to-noise ratio (SNR) of 20 is used. This is an amplitude ratio, i.e., when the noise variance is unity, the signal amplitude is simply SNR. Results shown in Fig. 4.6 indicates that large sidelobes result from noisy measurements. This is due to the inherent form of the pseudoinversion shown in (2.12), where a small singular value (σ_j) can cause a small variation in y to become a large variation in x.

In order to reduce the noise effect, we apply the regularized pseudoinversion filter. Notice that in this case we do not arrive at an exact solution for $y = Qx$; instead, we obtain a solution which also pays attention to the smoothness of x via the penalty term using the norm of x. Because our measurements are corrupted with correlation noise, the regularized estimate is obtained via (3.15) and (3.18).

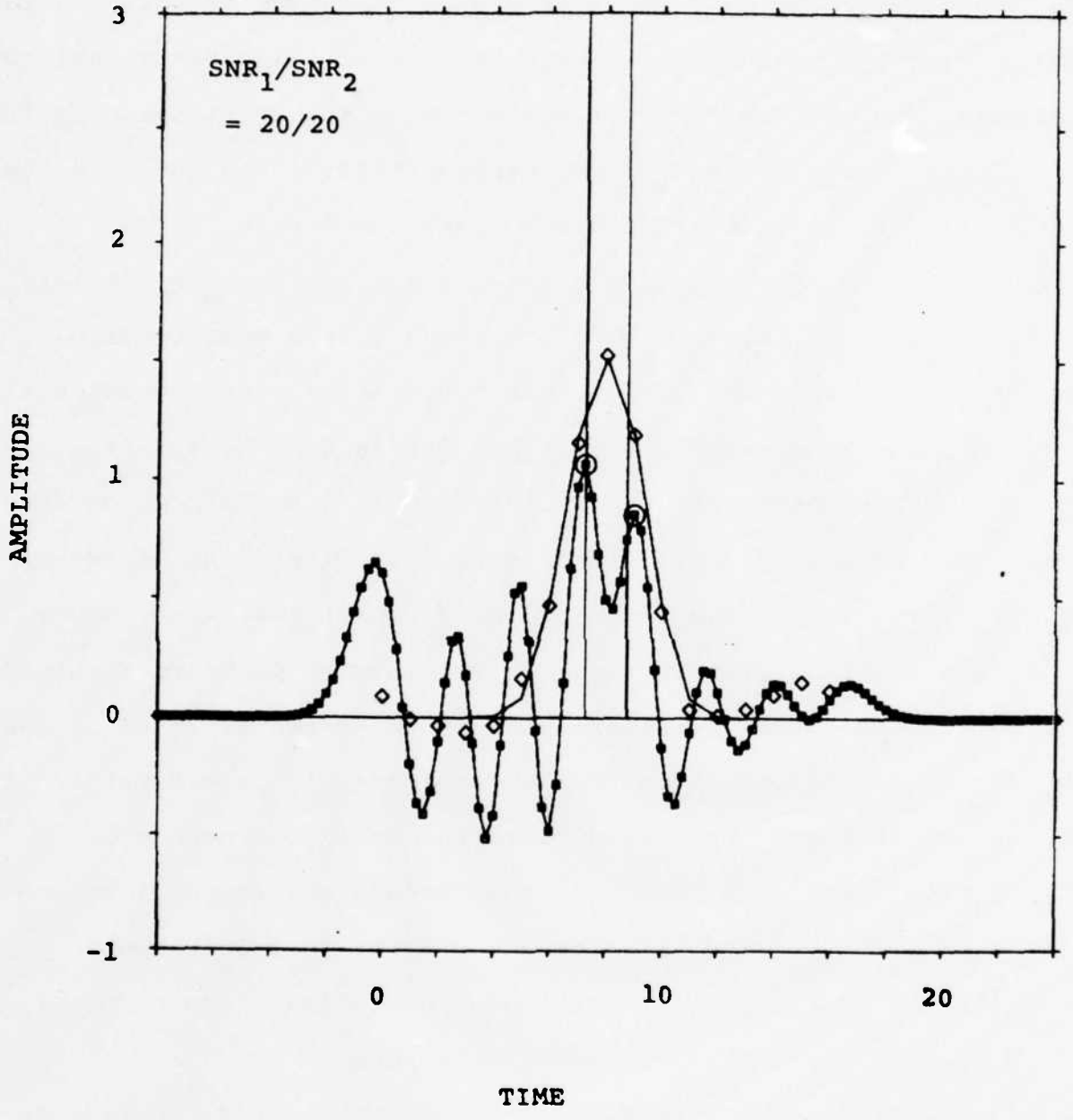

Fig. 4.6. Two-target with noisy measurements, no regularization.

The results are given in Fig. 4.7. Notice that the regularization factor can substantially reduce the noise effect. In this case, the ϵ is choosen to be a tenth of the inverse signal-to-noise ratio. For SNR=20, ϵ=.005. With the regularization factor included, the pseudoinversion filter also includes the normalization using the noise covariance matrix.

Also shown in Fig. 4.7 is a algorithm for identifying scattering centers (targets) imbedded in the measurements. This algorithm is a "peak-picker" operating over the interval where the measurements are significantly above noise (i.e., for estimates higher than the two horizontal lines at the outside of the mainlobe). All peaks identified within that interval are further screened based on their amplitudes. Only those peaks within a certain range of the largest peak are retained (i.e., the lower horizontal line in the center). This is done to reduce sensitivities to the sidelobes of the estimates. The number of peaks identified gives the estimated number of targets. The peak locations then become the target location estimates. Because the recovered signal is a continuous function of time, the target location estimate can be nearly made free of sampling granularity errors.

We use Figs. 4.8-4.11 to further study the effects of sampling interval and noisy measurements. Recall that results

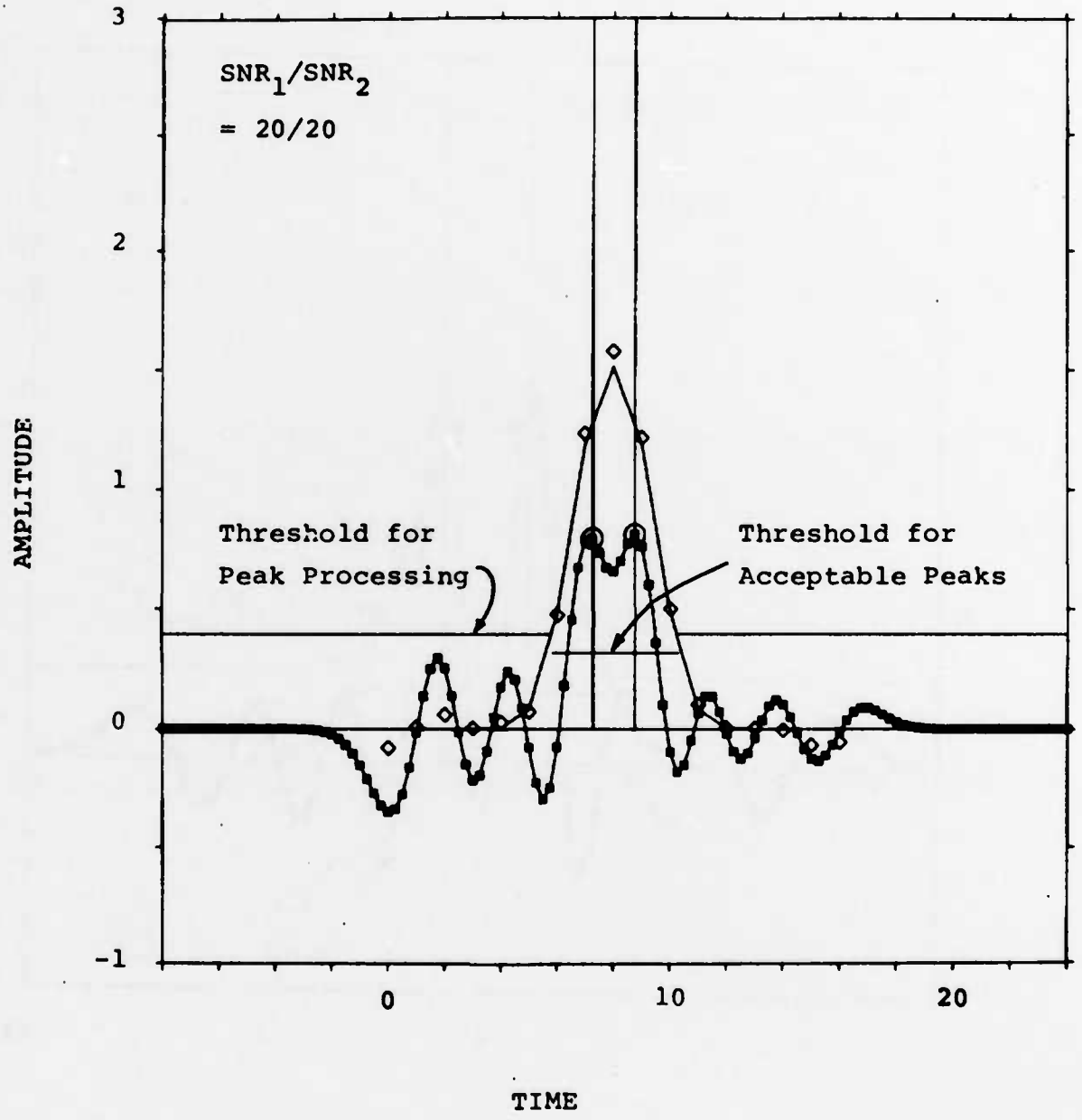

Fig. 4.7. Two-target with noisy measurements, with regularization.

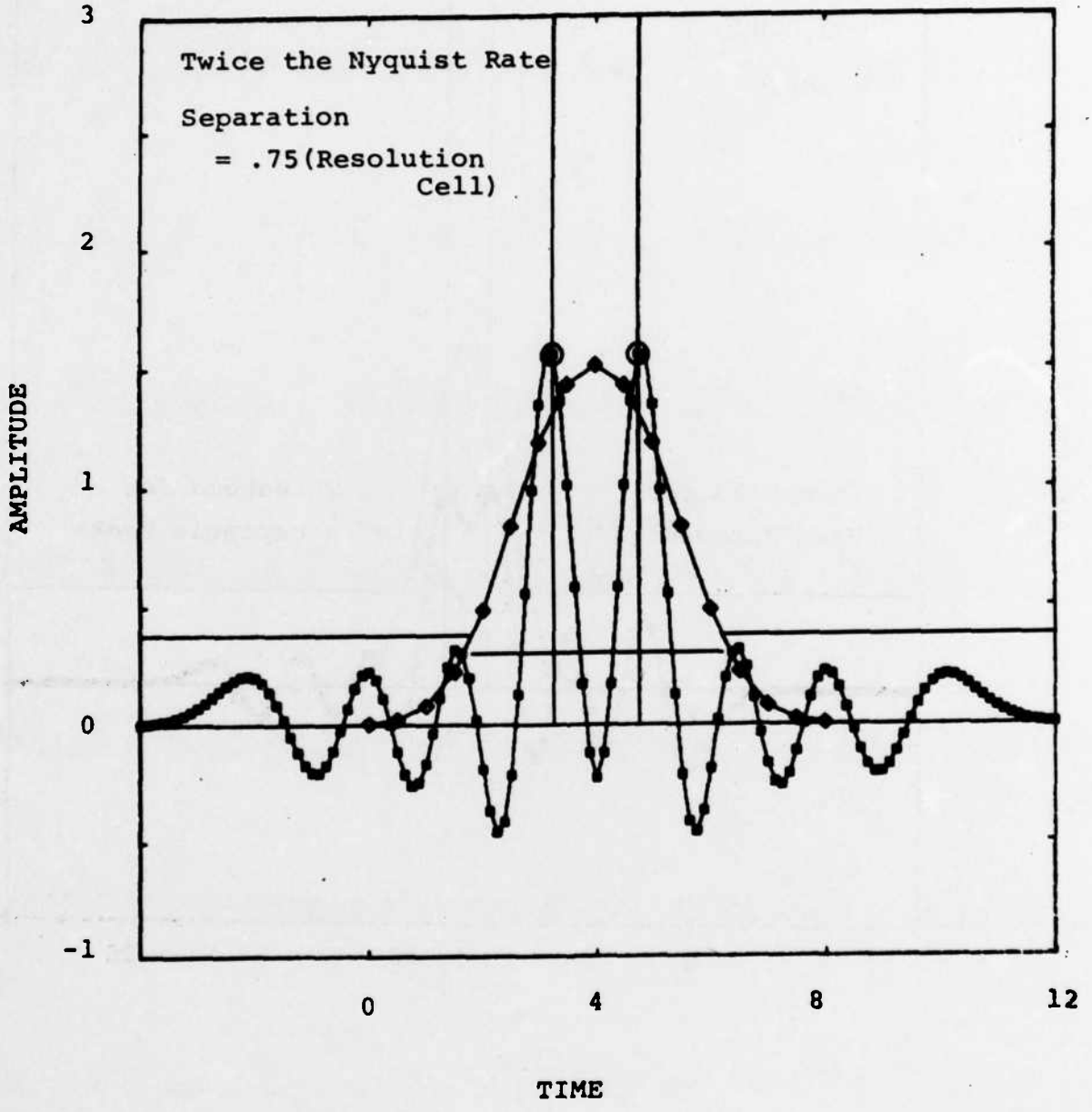

Fig. 4.8. Two-target case, noise free with twice the Nyquist rate ($\Delta t = 1/2$).

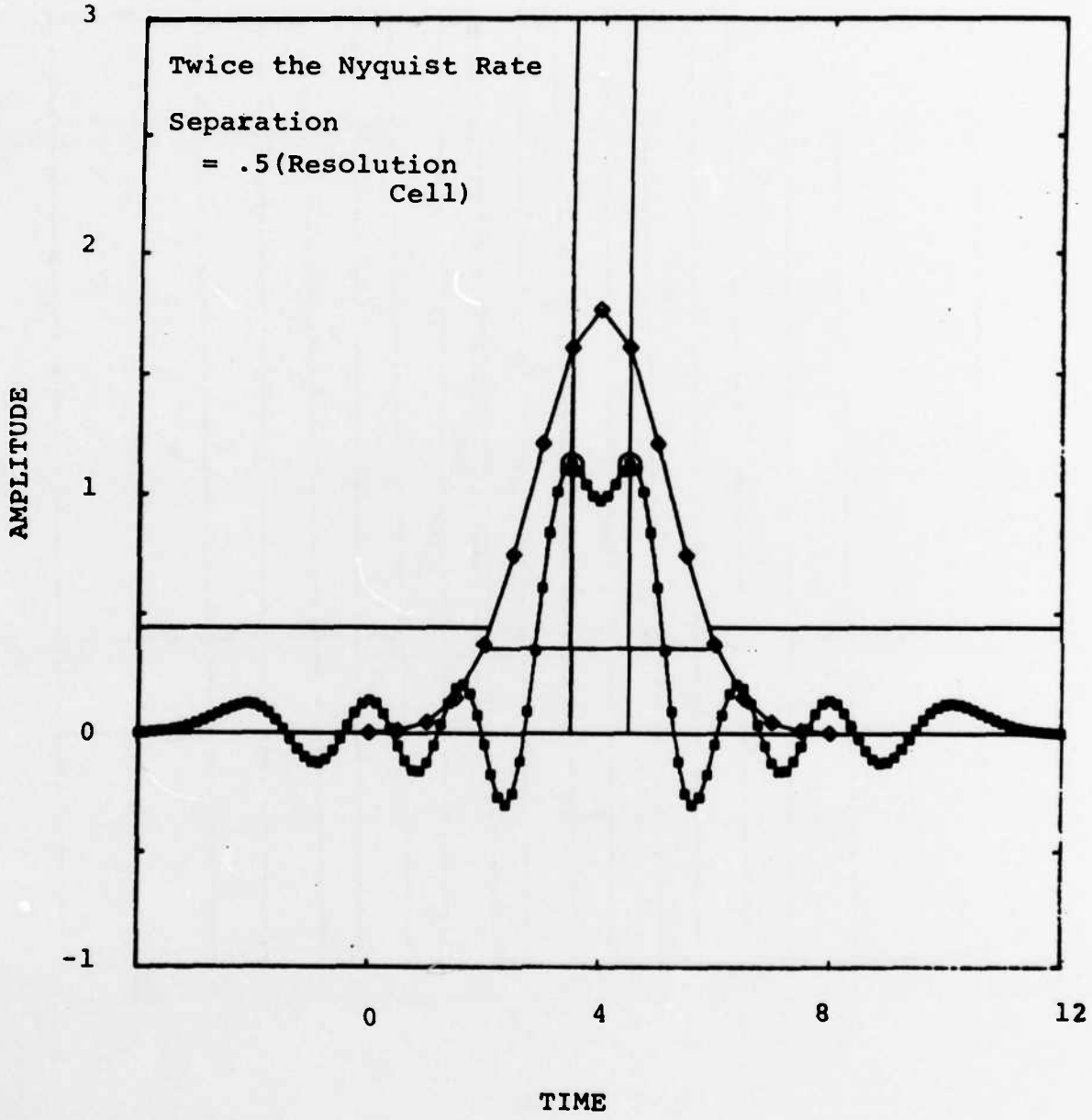

Fig. 4.9. Two-target case, noise free with twice the Nyquist rate and 1/2 resolution cell separation.

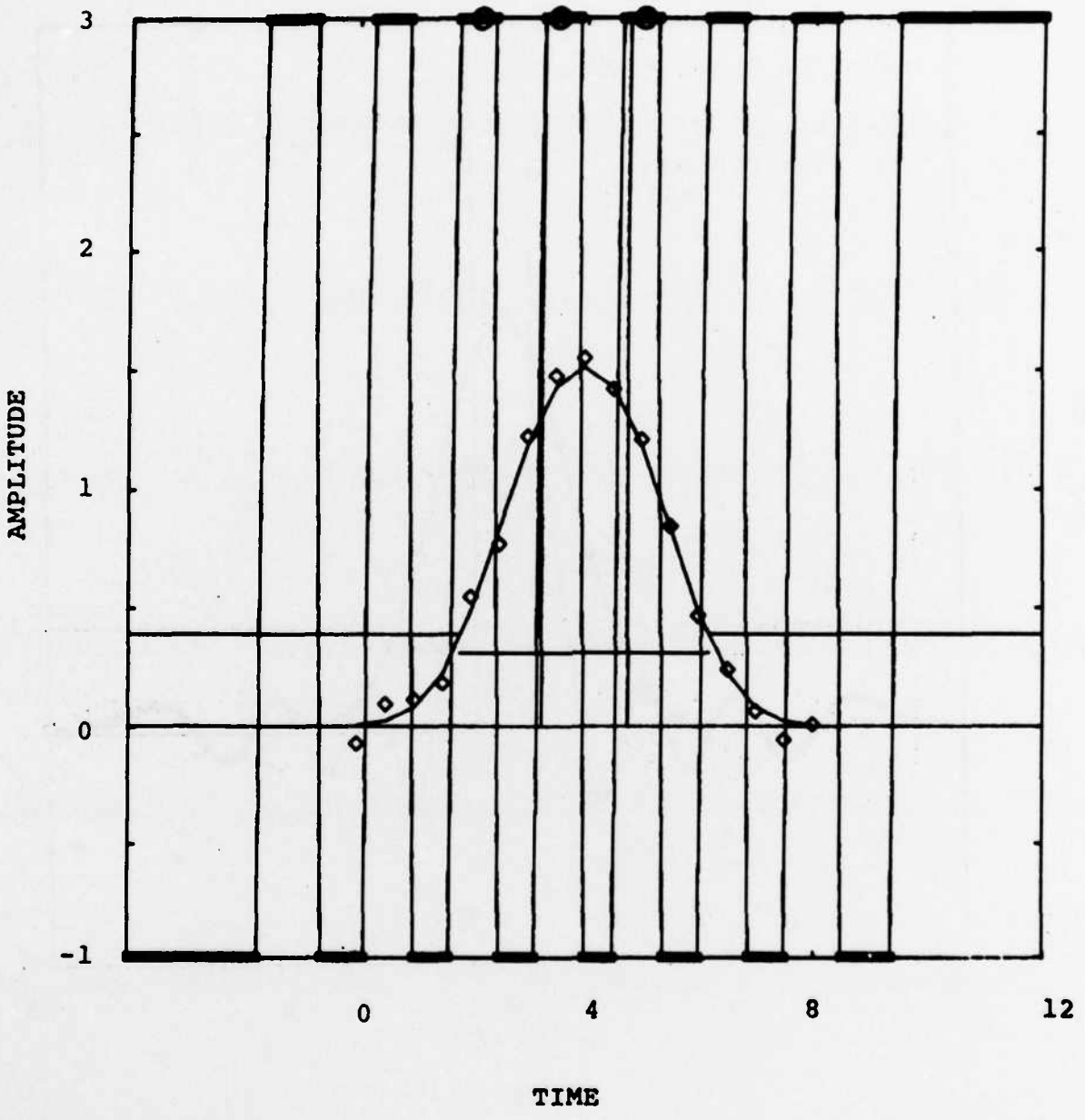

Fig. 4.10. Two-target case, noisy data with twice the Nyquist rate and 1/2 resolution all separation.

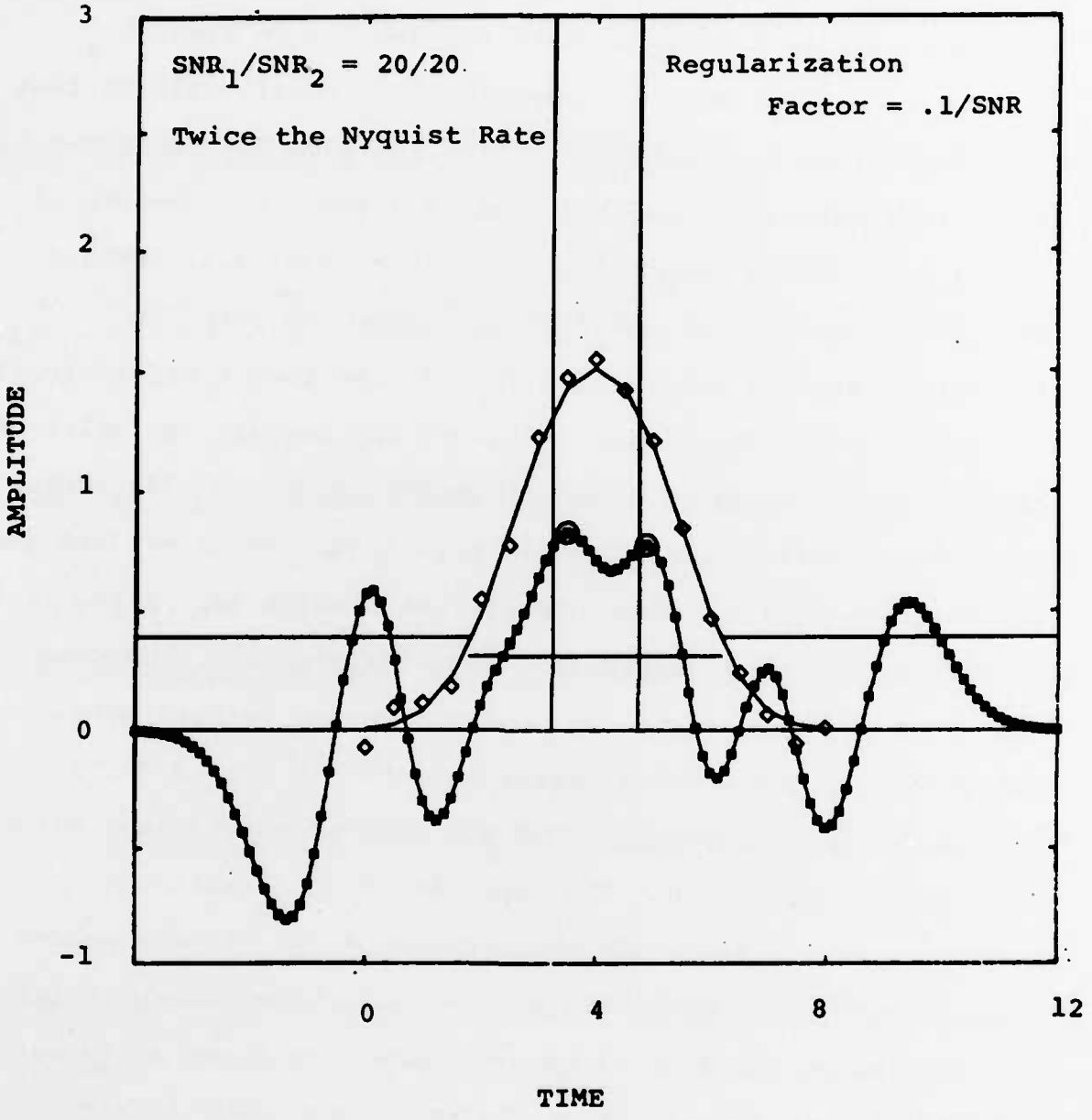

Fig. 4.11. The same conditions as Fig. 4.10 except with regularization in the filter.

of Figs. 4.4-4.7 used the "Nyquist" sampling interval (=1). This interval is reduced to half for results in Figs. 4.8-4.11. We have also enlarged the horizontal scale so that the interval between samples remains the same for the figures. Noise-free data were used for Figs. 4.8 and 4.9. Results of Fig. 4.8 should be compared with those of Fig. 4.5. Notice that the resolution is substantially improved with the increased sampling rate. In Fig. 4.9, the target separation is reduced to a 1/2 resolution cell, yet two targets can still be clearly seen. Noisy samples with a SNR of 20 and .75 resolution cell separation are used in Fig. 4.10. It is evident that the pseudoinversion filter now acts as a noise amplifier. This is because when the samples are taken closer, the condition number of QQ^* also increases, and the result becomes more suseptible to measurement perturbations. In Fig. 4.11, a regularization factor of .1/SNR was applied to the same set of data used in Fig. 4.10. The improvement is dramatic.

We now study the performance of the closely spaced objects resolution problem statistically. The probabilities of correct indentification of target numbers in terms of target separation with target SNR as parameter are shown in Fig. 4.12. These results are obained with 100 Monte Carlo repetitions. A regularization parameter of $\varepsilon = .1/SNR$ was used for all these results. This parameter was chosen to insure a

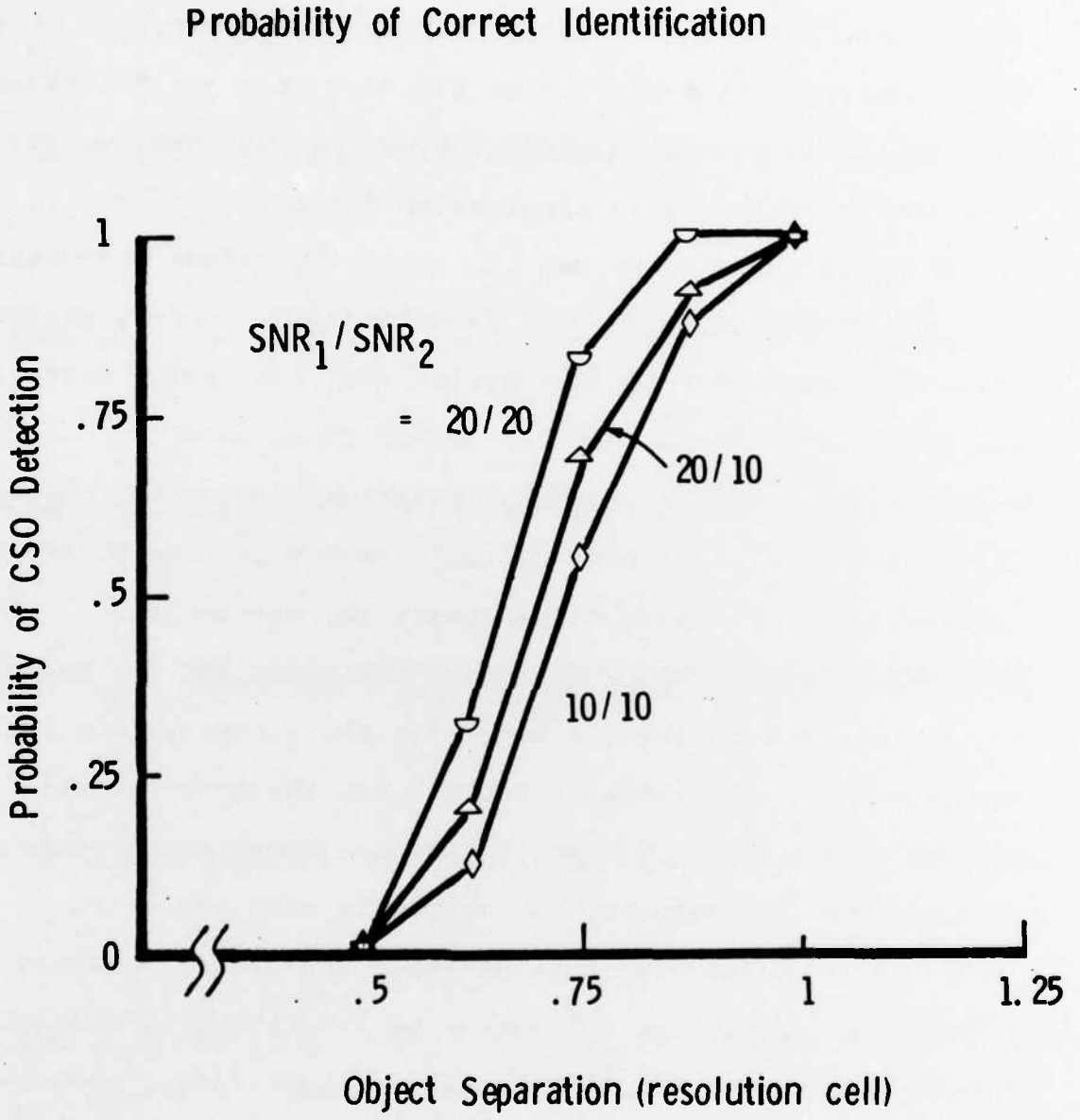

Fig. 4.12. Probability of correctly identifying two targets in a cluster.

less than 1% false alarm probability for a point target. We remark that although techniques for realtime selection of ε based upon the residuals and/or the norm of x are available and implemented in many scientific subroutine packages, we believe that the above choice is application dependent and a pre-selected coefficient can substantially reduce computational burden. Comparing these with results of [6] where a maximum likelihood estimator in conjunction with the Akaiki criterion was used, it is found that our method gives poorer performances. This is somewhat expected bacause the method of [6] is parametric and near optimum (except the use of Akaiki information). Although our estimate is optimum, the identification procedure is rather arbitrary and furthermore we do not assume a parametric model for the targets. Our results are, however, substantially better than the conventional rule-of-thumb resolution criterion, i.e., one resolution cell separation. Furthermore, our method is much easier to implement compared with that of [6]. The target location estimation accuracy as a function of separation to a nearby interfering target for a two-equal-ampltude-target model with SNR of 20 is shown in Fig. 4.13.

Also traced is the analytical model given in [7]. The model of [7] is based upon the Cramer-Rao bound analysis for unbiased

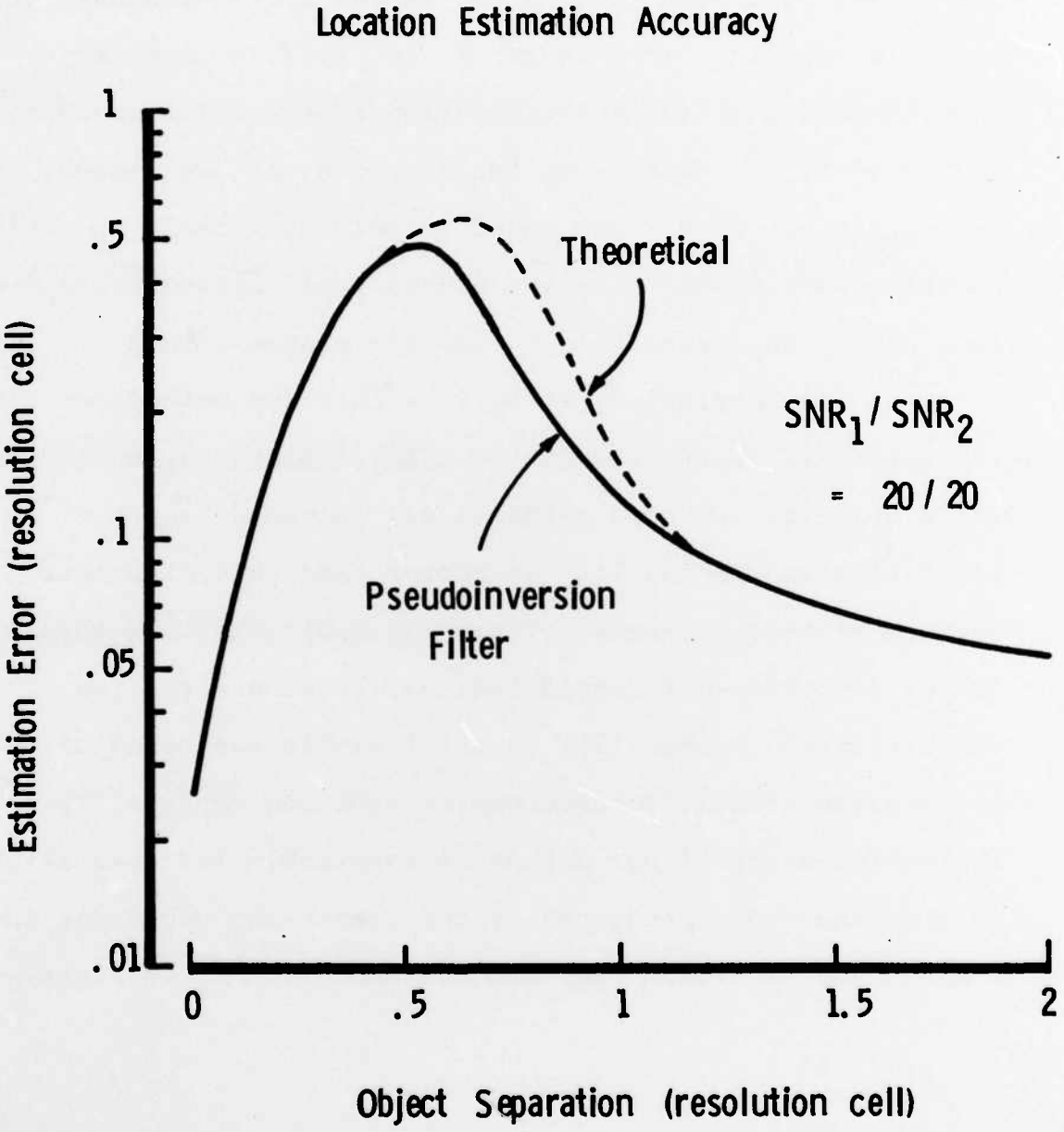

Fig. 4.13. Location estimation accuracy.

estimates together with a bias model for the case when targets are unresolved. The total error is the root-sum-square of these two errors. The result of Fig. 4.13 is somewhat suprising because our error is slightly smaller than that indicated by the Cramer-Rao bound over a certain region. This is because the Cramer-Rao bound is only applicable to unbiased estimates while our estimates are slightly biased (away from each other) thus resulting in smaller random errors.

In conclusion, we believe that the method described above is very attractive for realtime implementation because of its simplicity and good performance. Although the identification probability is poorer than that of a near optimum algorithm, its simplicity in implementation should be a factor for trade-off considerations. Furthermore, the identification probability is still within the bound of performance usually considered for realtime systems [7]. The estimation error of our method is comparable and even slightly smaller than that predicted by the Cramer-Rao bound due to the existance of a slight bias error.

V. CONCLUDING REMARKS

In this report, we applied the pseudoinversion operator to the estimation of linear systems (or input functions) with discrete measurements. Relevant operator theory was first reviewed. Theorems were stated with outlines of, or references cited for, their proofs. The solution to the problem of scattering function estimation was explicitly given. Three examples were presented to illustrate our results. In one example, an interpolation formula for finite number of samples was given. This result is the time domain counterpart of the Modified Discrete Fourier Transform known in the literature. In another example, the problem of closely spaced targets (signals) resolution was studied.

Since the pseudoinversion involves matrix inversion, numerical problems may exist for some problems. Methods such as truncated or filtered singular value decomposition and regularization can be applied. General techniques for selecting a truncation or regularization are available, while otners may be very specific to particular applications.

ACKNOWLEDGMENTS

The authors would like to thank L. Youens for preparing numerical results of this report. The skillful typing and patience of Christine Tisdale were also essential in preparation of the manuscript.

REFERENCES

1. I. Gohberg and S. Goldberg, Basic Operator Theory (Birkhauser, Boston, 1981).

2. B. R. Hunt, "Biased Estimation for Nonparametric Identification of Linear Systems," Mathematical Biosciences 10, p. 215-237, (1971).

3. C. Byrne and R. M. Fitzgerald, "A Unifying Model for Spectral Estimation ," Proc. RADC Spectrum Estimation Workshop, p. 157-162, 1979.

4. C. W. Groetsch, Generalized Inverses of Operators: Representation and Approximation (Dekker, New York, 1977).

5. J. Cullum, "Ill-posed Problems, Regularization and Singular Value Decomposition," Proc. 19th IEEE Conf. on Decision and Control, Albuquerque, NM, 1980, p. 29-35.

6. M. J. Tsai, "Simulation Study on Detection and Estimation of Closely Spaced Optical Targets," Technical Note 1980-19, M.I.T. Lincoln Laboratory, (18 March 1980), DTIC AD-A088098/9.

7. C. B. Chang and K. P. Dunn, "A Functional Model for the Closely Spaced Object Resolution Process," Technical Report 611, M.I.T. Lincoln Laboratory (20 May 1982), DTIC AD-A116890.

UNCLASSIFIED

SECURITY CLASSIFICATION OF THIS PAGE *(When Data Entered)*

REPORT DOCUMENTATION PAGE		READ INSTRUCTIONS BEFORE COMPLETING FORM
1. REPORT NUMBER ESD-TR-83-038	2. GOVT ACCESSION NO. A132283	3. RECIPIENT'S CATALOG NUMBER
4. TITLE *(and Subtitle)* Application of Pseudoinversion to Linear System Identification with Discrete Measurements		5. TYPE OF REPORT & PERIOD COVERED Technical Report 6. PERFORMING ORG. REPORT NUMBER Technical Report 629
7. AUTHOR(s) Chaw-Bing Chang and Richard B. Holmes		8. CONTRACT OR GRANT NUMBER(s) F19628-80-C-0002
9. PERFORMING ORGANIZATION NAME AND ADDRESS Lincoln Laboratory, M.I.T. P.O. Box 73 Lexington, MA 02173-0073		10. PROGRAM ELEMENT, PROJECT, TASK AREA & WORK UNIT NUMBERS Program Element No. 63304A and 63308A
11. CONTROLLING OFFICE NAME AND ADDRESS Ballistic Missile Defense Program Office Department of the Army 5001 Eisenhower Avenue Alexandria, VA 22333		12. REPORT DATE 15 July 1983 13. NUMBER OF PAGES 56
14. MONITORING AGENCY NAME & ADDRESS *(if different from Controlling Office)* Electronic Systems Division Hanscom AFB, MA 01731		15. SECURITY CLASS. *(of this report)* Unclassified 15a. DECLASSIFICATION DOWNGRADING SCHEDULE

16. DISTRIBUTION STATEMENT *(of this Report)*

Approved for public release; distribution unlimited.

17. DISTRIBUTION STATEMENT *(of the abstract entered in Block 20, if different from Report)*

18. SUPPLEMENTARY NOTES

None

19. KEY WORDS *(Continue on reverse side if necessary and identify by block number)*

pseudoinverse
compact operator
linear system identification
nonparametric estimator
modified discrete Fourier transform
closely spaced object resolution
radar/optical signal processing

20. ABSTRACT *(Continue on reverse side if necessary and identify by block number)*

Formulas for the pseudoinverse of a compact operator are applied to linear system identification and scattering function estimation from a finite set of noisy measurements. The result is a nonparametric estimator possessing several desirable features. The approach encompasses the Modified Discrete Fourier Transform and is applied herein to the important problem of closely spaced object resolution in radar/optical signal processing.

DD FORM 1 Jan 73 1473 EDITION OF 1 NOV 65 IS OBSOLETE

UNCLASSIFIED

SECURITY CLASSIFICATION OF THIS PAGE *(When Data Entered)*

END

FILMED

9-83

DTIC